



CrossMark
 click for updates

Cite this: *RSC Adv.*, 2014, 4, 39214

Design, synthesis, evaluation and 3D-QSAR analysis of benzosulfonamide benzenesulfonates as potent and selective inhibitors of MMP-2

Han-Yue Qiu,† Zhong-Chang Wang,† Peng-Fei Wang,† Xiao-Qiang Yan, Xiao-Ming Wang,* Yong-Hua Yang* and Hai-Liang Zhu*

A novel series of MMPis was designed, synthesized and purified using a scaffold modification strategy. The new compounds were also evaluated for biological activity against A549, MCF-7, HepG2 and Hela as potential inhibitors of MMP-2. The most potent inhibitor against MMP-2 was compound **19** ($IC_{50} = 0.38 \mu M$). Its antitumor effect is believed to be due to the induction of apoptosis, which is further confirmed by Annexin V-FITC/PI staining assay using flow cytometry analysis. Furthermore, all the compounds were evaluated for cytotoxicity against 293T. In addition, 3D-QSAR studies were conducted. The result showed that the benzosulfonamide benzenesulfonate MMPis may prove interesting lead candidates to target MMP-2 associated tumor, where the MMP-2 domain is located extracellularly.

Received 8th July 2014
 Accepted 15th August 2014

DOI: 10.1039/c4ra06438k

www.rsc.org/advances

1 Introduction

Matrix metalloproteinases (MMPs) are a family of more than 28 subtypes of zinc- and calcium-dependent endopeptidases involved in the degradation of all components of the extracellular matrix (ECM).^{1–3} MMPs play a crucial role in physiological tissue remodeling and repair and continue to be an interesting target for drug discovery.^{4–6} However, aberrant recruitment of MMPs can lead to tissue degradation, which has been linked to several disease states, such as tumor growth and metastasis.⁶ Under normal physiological conditions, endogenous tissue inhibitors of MMPs (TIMPs) could serve as effective anticancer agents.^{7,8} In addition to other direct TIMP/MMP interactions, the TIMPs also coordinate to the catalytic zinc ion of the MMPs and as a result control their activity.⁹ Overexpression of MMPs, or inadequate control by TIMPs, has been observed and implicated with a variety of chronic diseases including cancers, arthritis and other illnesses.¹⁰ Therefore, there has been significant interest in the development of specific inhibitors to deal with this problem.¹¹

The development of low molecular weight synthetic inhibitors of MMPs is an attractive approach to the therapeutic treatment of a variety of diseases, such as arthritis and cancer.^{12–17} Especially, inhibitors of MMP-2 are sought for prevention of cancer tumor growth.¹⁸ Consequently, many potent and orally active broad-spectrum MMP inhibitors, active against a range of different enzymes, or of selective inhibition,

were discovered during the past decade, some of which having been in clinical trials. MMP inhibitors A–H (ref. 8,19–21) were tested against cancers; MMP inhibitors I (cipemastat)²² and J (illomastat)²³ were tried in the clinics for inflammation (Fig. 1). Unfortunately, these broad-spectrum MMP inhibitors have been limited by non-specificity and thus non-selective toxicity and dose-limiting efficacy.²⁴ Still, it was thought that the inhibition of MMPs may cause undesirable side effects.²⁵ As a consequence, no MMP inhibitor has emerged on the market.⁸ To solve this problem, we targeted our efforts toward the discovery of new chelating groups suitable for MMP inhibitor templates.^{26,27} Structural studies have revealed that most inhibitors interact with the MMP active site residues through an elaborate hydrogen-bond network and chelation of the active-site zinc.² Several zinc binding groups (ZBG) have been discovered, which include secondary amines, amides, imines, imidazoles, carboxylates, aminocarboxylates, sulfhydryls, hydroxamates, phosphonates and phosphinates.^{28–32} In recent years, interest in benzosulfonamides has been increased due to their high biological activity, however the broad-benzosulfonamides as MMP inhibitors,³³ hitherto have not been recognized.

Our work has been focused on metastasis formation in which MMPs (especially MMP-2) have a vital role by mediating tumor cell dissemination. Efficient inhibition to MMPs is, therefore, an important therapeutic approach, which has attracted considerable attention within academia and industry for the last two decades or so. We now describe the structure-based design and synthesis of novel, potent, and selective MMP-2 inhibitors that utilize benzosulfonamide benzenesulfonates as a scaffold.

State Key Laboratory of Pharmaceutical Biotechnology, Nanjing University, Nanjing 210093, People's Republic of China. E-mail: zhuhl@nju.edu.cn; yangyh@nju.edu.cn; Fax: +86-25-83592672; Tel: +86-25-83592672

† These three authors equally contributed to this paper.

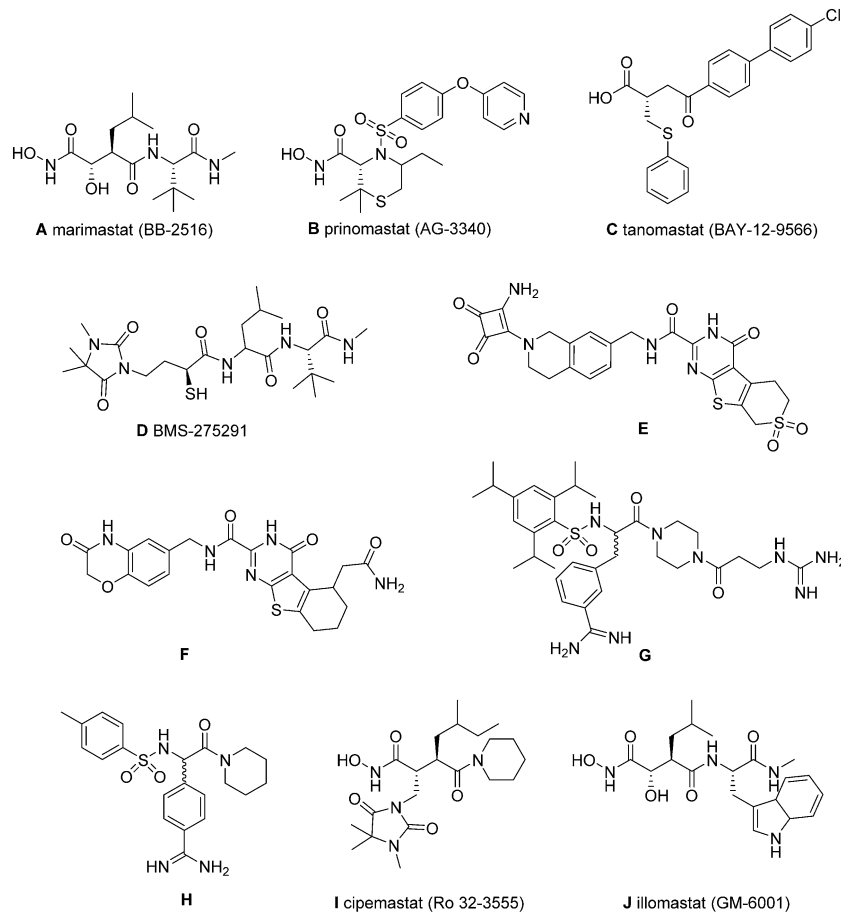
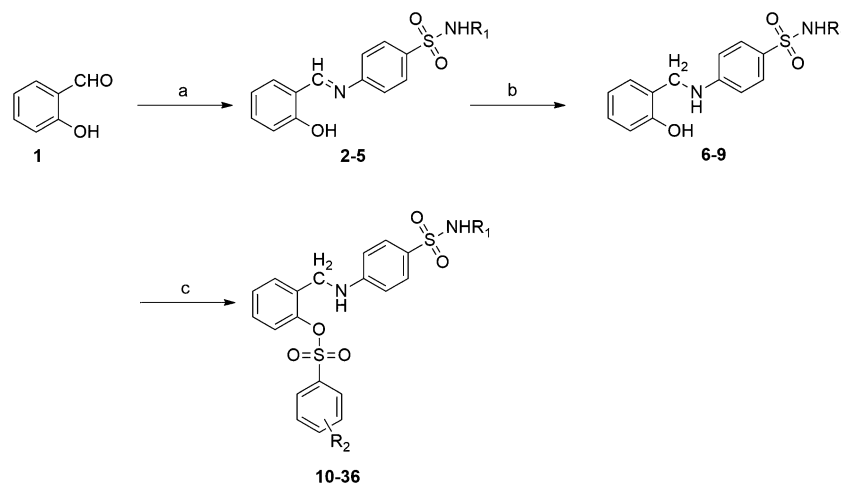


Fig. 1 Selected MMP inhibitors.



Scheme 1 General synthesis of compounds (10–36). Reagents and conditions: (a) 1.0 equiv. *p*-R₁NHSO₂PhNH₂, CH₃CH₂OH, reflux 2–4 h, 80.3–87.8%; (b) 1.0 equiv., NaBH₄, CH₃CH₂OH, 0 °C 2 h, 83.2–87.4%; (c) 2.0 equiv., ArSO₂Cl, 0 °C 10 h, 41.9–66.3%.

2 Results and discussion

2.1 Chemistry

The synthetic route followed for the synthesis of twenty-seven target compounds is depicted in Scheme 1. To a stirred solution

of the sulfonamide derivative and salicylaldehyde in ethanol, glacial acetic acid was added as catalyst. The reaction mixture was stirred for 4 h to give the Schiff bases 2–5, in high yields (80.3–87.8%). The Schiff bases were then treated with NaBH₄ to afford compounds 6–9 and subsequently these compounds

Table 1 Crystal data for compound 10 and 16

Compound	10	16
Empirical formula	C ₁₉ H ₁₈ N ₂ O ₅ S ₂	C ₂₁ H ₁₉ BrN ₂ O ₆ S ₂
Formula weight	418.1	538.0
Temperature (K)	273(2)	296(2)
Crystal system	Monoclinic	Triclinic
Space group	<i>P</i> 2 ₁ / <i>c</i>	<i>P</i> $\bar{1}$
<i>a</i> (Å)	8.2199(10)	20.976(2)
<i>b</i> (Å)	11.2497(14)	7.4910(9)
<i>c</i> (Å)	11.8661(14)	13.8228(14)
α (°)	70.477(3)	90.00
β (°)	71.107(3)	109.011(3)
γ (°)	82.365(4)	90.00
<i>V</i> (Å ³)	978.1(2)	2053.5(4)
<i>Z</i>	13	27
D _{calc} /g cm ⁻³	1.657	1.639
θ Rang (deg)	2.62–27.57	2.05–25.09
<i>F</i> (000)	494	1026
Reflections collected	10313	18744
Data/restraints/parameters	4379/0/261	3649/0/288
Absorption coefficient (mm ⁻¹)	0.792	0.784
<i>R</i> ₁ ; <i>wR</i> ₂ [<i>I</i> > 2 σ (<i>I</i>)]	0.0407/0.1027	0.0353/0.0891
<i>R</i> ₁ ; <i>wR</i> ₂ (all data)	0.0528/0.1101	0.0458/0.0956
GOF	1.038	1.039
Larg. peak/hole (e Å ⁻³)	0.350/−0.326	0.255/−0.286

were coupled with the appropriate substituted benzenesulfonyl chloride to give the target compounds, using triethylamine (TEA) as the deacid reagent. All of the target compounds 10–36 are reported for the first time, and gave satisfactory analytical and spectroscopic data. ¹HNMR and ESI-MS spectra were consistent with the assigned structures.

2.2 Crystal structures of compound 10 and 16

Among these compounds, the crystal structures of compound 10 and 16 were determined by X-ray diffraction analysis. The crystallographic data for the structural analysis are presented in Table 1, and their 3D images with the atomic labeling system are shown in Fig. 2.

2.3 Biological activity

2.3.1 MMP-2 inhibitory activity. All the compounds were tested for their inhibition to MMP-2, with CMT-1 as the positive

control drug. In this assay, the IC₅₀ values of the new compounds, possessing sufficiently potent anticancer activity, are shown in Table 2; the results were compared with that shown by the anticancer drug CMT-1, under identical conditions, and it was revealed that most of the synthesized compounds exhibited significant anticancer activities.

The MMP-2 was inhibited by compounds 10–36 with IC₅₀ in the range of 0.38–68.23 μ M. Compound 19 was the most active having an IC₅₀ value of 0.38 μ M, whereas compound 22 was the least active with IC₅₀ value of 68.23 μ M (Table 2). Different substituents of benzoic acid benzene ester have been chosen as the research object and the results showed that the compounds with substituents at the *para*-position are more potent than those bearing *meta*-position substituents (such as 12 and 16); it was also found that the electron-withdrawing group of R₂ was essential to improve the inhibitory activity, and the inhibitory activities increased in the following order: CH₃ < H < Br < Cl < F < NO₂. Provided that the benoic acid methyl ester group was kept unchanged, the effect of changing different sulfanilamide derivatives was subtle, and compounds 12 and 19 were identified as the most potent inhibitors.

In comparison, we found that these compounds, with bulky and electron-withdrawing groups on the benzene ring (such as NO₂), exhibited more potent anticancer activities than those having electron-donating substituents (such as CH₃). From the abovementioned observation, it was concluded that the compounds with a nitro or halogen substituted benzene ring were the most potent.

2.3.2 Antiproliferation assay. In order to test the antiproliferation activity of the new compounds, we evaluated them against A549, MCF-7, HepG2 and Hela in comparison to the known anticancer drugs, **Gefitinib** and **Celecoxib**. The results are summarized in Table 2. Most of the new synthetic salicylaldehyde sulfonamide derivatives, containing the benzene sulfonic acid benzyl ester group exhibited remarkable antiproliferative activity. Especially on antiproliferation against Hela cells, compounds 19, 25, 32 and 33 showed better activity than the positive control. From the analysis of these test results, a conclusion can be drawn: strong R₂ electron-withdrawing substituents on the benzene ring, (NO₂ and F, for example) endow compounds with more potent activities than those with electron-donating groups.

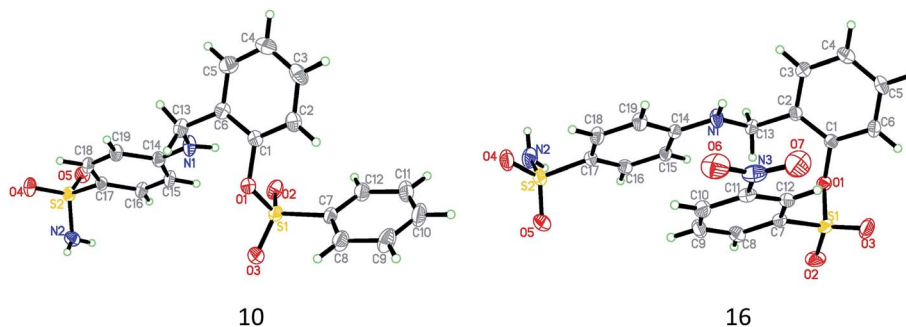


Fig. 2 Crystal structure diagrams of compound 10 and 16.

Table 2 Biological activities (IC₅₀, μM) of target compounds (10–36)

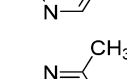
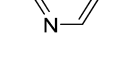
Compounds	R ₁	R ₂	IC ₅₀ ^a (μM)	IC ₅₀ ^c (μM)			
			MCF-7 ^b	HepG2 ^b	HeLa ^b	A549 ^b	MMP-2 ^d
10	H	<i>p</i> -H	12.04	13.83	6.21	8.28	50.82
11	H	<i>p</i> -CH ₃	13.21	17.61	8.55	11.2	23.43
12	H	<i>p</i> -NO ₂	9.45	2.02	2.69	4.23	1.22
13	H	<i>p</i> -F	9.87	4.21	7.11	6.73	6.80
14	H	<i>p</i> -Cl	11.26	4.52	10.13	5.47	29.24
15	H	<i>p</i> -Br	17.91	7.27	14.41	8.11	49.63
16	H	<i>m</i> -NO ₂	20.41	8.38	10.95	12.9	18.26
17		<i>p</i> -H	4.46	12.0	4.33	3.41	5.26
18		<i>p</i> -CH ₃	8.27	16.88	5.89	4.42	11.63
19		<i>p</i> -NO ₂	1.78	2.62	0.63	1.17	0.38
20		<i>p</i> -F	2.99	4.68	1.78	2.31	16.20
21		<i>p</i> -Cl	4.51	7.21	3.45	6.14	24.54
22		<i>p</i> -Br	5.38	8.78	5.1	8.17	68.23
23		<i>m</i> -NO ₂	10.9	11.9	8.42	10.1	12.32
24		<i>p</i> -CH ₃	5.11	21.7	1.16	7.4	62.60
25		<i>p</i> -NO ₂	0.99	3.61	0.96	2.11	13.24
26		<i>p</i> -F	1.71	6.63	3.72	5.75	28.10
27		<i>p</i> -Cl	4.12	8.2	6.11	8.34	36.81
28		<i>p</i> -Br	8.17	9.91	5.09	10.1	49.83
29		<i>m</i> -NO ₂	10.11	16.53	7.02	11.2	34.20
30		<i>p</i> -H	6.31	6.7	5.71	3.32	26.53
31		<i>p</i> -CH ₃	7.11	6.81	7.85	2.91	56.61

Table 2 (Contd.)

Compounds	R ₁	R ₂	IC ₅₀ ^a (μM)	IC ₅₀ ^c (μM)			
			MCF-7 ^b	HepG2 ^b	HeLa ^b	A549 ^b	MMP-2 ^d
32		<i>p</i> -NO ₂	1.53	0.81	0.44	1.19	9.83
33		<i>p</i> -F	2.72	4.93	0.97	3.53	11.62
34		<i>p</i> -Cl	4.95	5.82	1.78	6.91	9.88
35		<i>p</i> -Br	8.31	5.06	4.23	7.53	42.36
36		<i>m</i> -NO ₂	11.6	9.21	3.21	10.33	16.54
Gefitinib	—	—	6.70	—	1.59	2.78	—
Celecoxib	—	—	7.01	0.68	7.51	2.21	—
CMT-1	—	—	—	—	—	—	1.20

^a Biological activity was measured using the MTT assay. Values are the average of three independent experiments run in triplicate. Variation was generally 5–10%. ^b Cancer cells kindly supplied by State Key Laboratory of Pharmaceutical Biotechnology, Nanjing University. ^c Errors were in the range of 5–10% of the reported values, from three different assays. ^d Human recombinant enzymes, by the esterase assay (4-nitrophenylacetate as substrate).

2.3.3 Cytotoxicity. All of the new compounds were evaluated for their toxicity against the human kidney epithelial cell 293T (median cytotoxic concentration (CC₅₀) data) using the MTT assay. As shown in Table 3, these compounds were tested at multiple doses to study the viability of 293T and demonstrated almost no cytotoxic activities *in vitro* against human kidney epithelial cell 293T.

2.3.4 Apoptosis assay. In order to decipher whether the inhibition of cell growth of HeLa is related to cell apoptosis, HeLa cell line apoptosis induced by compound **19** was determined using flow cytometry. The results are shown in Fig. 3; the percentage of apoptotic cells was markedly elevated in a dose-dependent manner. The percentages of cell apoptosis 3.12%, 8.12%, 16.81%, 62.74% correspond to the concentration of compound **19** 0, 2, 8 and 32 μM, respectively.

2.4 Molecular docking

Docking study was performed aiming at fitting compound **19** into the active center of the matrix metalloproteinases MMP-2 (PDB code: 1QIB).³⁴ The results obtained are presented in the two groups of pictures: Fig. 4 and 5 show that the binding mode of compound **19** results from its interaction with 1QIB protein. The docking results revealed that four amino acids **TYR155**, **GLY152**, **ARG148** and **GLU150** located in the binding pocket of

protein played major roles in binding to compound **19**, *via* two hydrogen bonds and two charge interactions (2D diagram). Compound **19** forms hydrogen bonds with the backbone NH of **TYR155** (angle O··H–N = 166.0°, distance = 2.2 Å), **GLY152** (angle O··H–H = 161.6°, distance = 2.9 Å); the atom on nitril contributes to the two charge interactions. Moreover, two coordinate bonds are formed between the zinc cation and oxygen atoms, as shown in Fig. 5, which seem to drastically increase the binding affinity. The molecular docking results, along with the biological assay data, suggest that compound **19** is a potential inhibitor of MMP-2.

2.5 3D-QSAR model

To obtain the systematic SAR profile of benzenesulfonamide benzenesulfonates, as antitumor agents and to explore more powerful and selective inhibitors of MMP-2, a 3D-QSAR model was built. By this effort, we intended to discuss the relationship of structure and activity, and cast a light on the discovery of more potent novel antagonists against MMP-2. This model was performed by built-in QSAR software of DS 3.5 (Discovery Studio 3.5, Accelrys, Co. Ltd), with all molecules converted to the active conformation and corresponding pIC₅₀ (μM) values, which were converted from the obtained IC₅₀ (μM) values of MMP-2 inhibition. These compounds were divided into a test set and a

Table 3 The median cytotoxic concentration (CC_{50}) data of all compounds

Compounds	CC_{50}^a , μM
10	59.00
11	62.29
12	56.43
13	56.76
14	49.28
15	74.63
16	52.49
17	51.30
18	46.79
19	51.90
20	59.25
21	58.31
22	57.75
23	50.09
24	53.31
25	50.74
26	45.19
27	66.49
28	57.34
29	49.76
30	57.48
31	63.93
32	49.19
33	49.91
34	54.67
35	47.60
36	44.76
Celecoxib	55.06

^a The cytotoxicity of each compound was expressed as the concentration of compound that reduced cell viability to 50% (CC_{50}).

training set, randomly. The test set composed of 22 agents and 5 agents were consisted of the relative training set, which are summarized in Table 4.

By default, the alignment conformation of each molecule possessed the lowest CDOCKER_INTERACTION_ENERGY among all of the docked poses. The critical regions (steric or electrostatic) affecting the binding affinity was gained by this 3D-QSAR model. Exerting CHARMM force field and PLS regression, the model was set up with conventional R^2 of 0.852, indicating that this model possesses good predicting capability. The relationship between observed and predicted values is shown graphically in Fig. 6.

All of the new molecules were aligned with the iso-surfaces of the 3D-QSAR model coefficients on electrostatic potential grids Fig. 7 (a) and van der Waals grids were listed (Fig. 7 (b)). The electrostatic map, depicted below, displays the favorable (in blue) or unfavorable (in red) electrostatic field regions in a contour plot, while the energy grids corresponding to the favorable (in green) or unfavorable (in yellow) steric effects are also marked out. Compounds showing strong van der Waals attraction in the green areas and a polar group in the blue electrostatic potential areas, are characterized as active. This model is in accordance with the actual situation for compounds under study. Thus, this model could provide a guideline to design and optimize more effective tubulin inhibitors and pave the way for us in further studies.

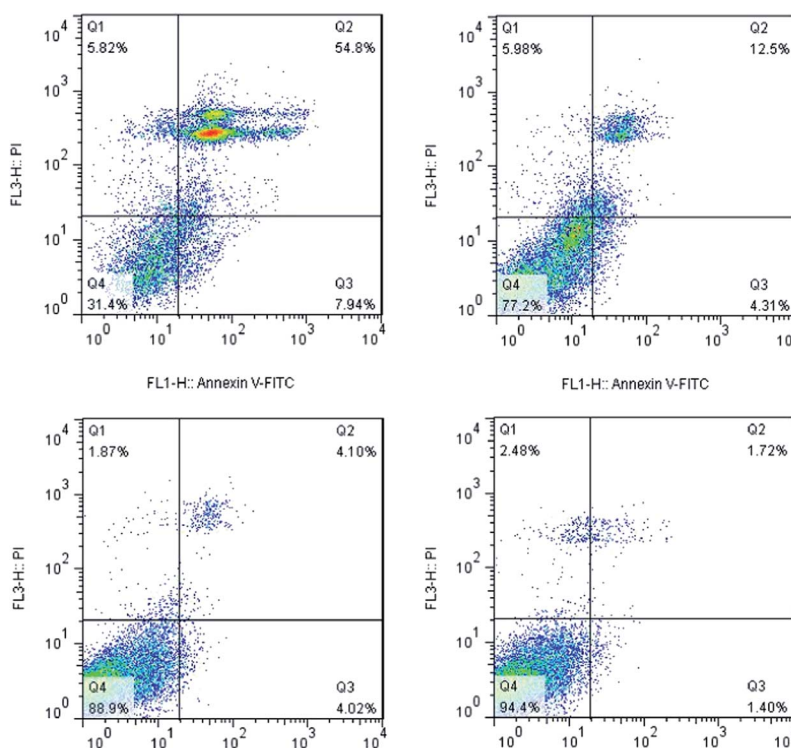


Fig. 3 Compound 19 induced apoptosis in HeLa cells with the density of 0, 2, 8, 32 μM . HeLa cells were treated with for 24 h. Values represent the mean \pm S.D, $n = 3$. $P < 0.05$ versus control. The percentage of cells in each part was indicated.

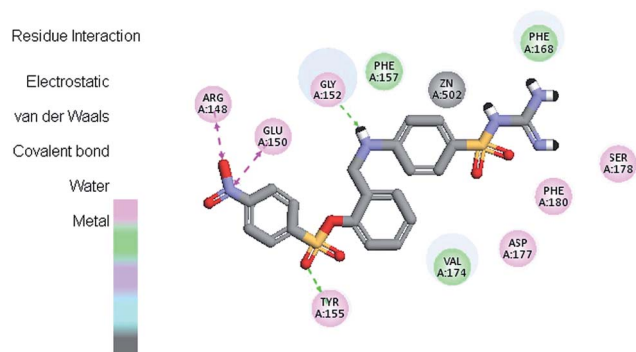


Fig. 4 Molecular docking 2D modeling of compound **19** with MMP-2: for clarity, only interacting residues are displayed.

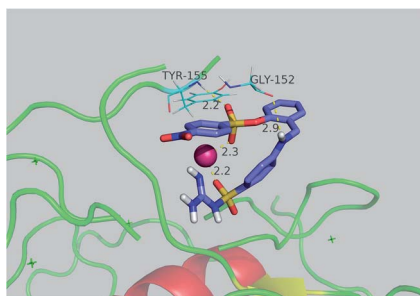


Fig. 5 Molecular docking 3D modeling of compound **19** with the MMP-2 binding site: for clarity, only interacting residues are displayed.

3 Conclusion

In a nutshell, a series of novel MMP-2 inhibitors (**10–36**) bearing the benzenesulfonate sulfonamide skeleton has been synthesized and evaluated for their biological activity. All of these compounds exhibited potent antiproliferation activities against HeLa and A549 cells and MMP-2 enzymatic inhibitory activities. Among them, **19** showed the highest inhibition activity against the growth of HeLa and A549 cell lines, with IC_{50} values of 0.63 and 1.17 μM and for MMP-2 the IC_{50} is 0.38 μM . More importantly, compound **19** exhibited almost no toxicity towards the human kidney epithelial cell 293T. In addition, the docking simulations which were performed, to find the probable binding models and poses, indicated that compound **19** can bind well with the MMP-2 active site. QSAR models were built with previous activity data and binding conformations and used as a reliable tool for the rational design of MMP-2 inhibitors.

4 Experiments

4.1 Materials and measurements

All chemicals and reagents used in current study were analytical grade. All the ^1H NMR spectra were recorded on a Bruker DPX 300 or 400 model Spectrometer in $\text{DMSO}-d_6$ and chemical shifts (δ) were reported as parts per million (ppm). ESI-MS spectra were recorded on a Mariner System 5304 Mass spectrometer. Melting points were determined on a XT4 MP apparatus (Taikhe Corp,

Table 4 Experimental, predicted inhibitory activity of compounds **10–36** by 3D-QSAR models based upon active conformation achieved by molecular docking

Compound ^a	MMP-2		Residual error
	Actual pIC_{50}	Predicted pIC_{50}	
10	4.29	4.50	−0.21
11	4.63	4.90	−0.27
12	5.92	5.89	0.03
13	5.17	5.00	0.17
14	4.53	4.78	−0.44
15	4.3	4.26	0.04
16	4.74	4.78	−0.04
17	5.28	5.04	0.24
18	4.94	4.96	−0.02
19	6.42	6.50	−0.08
20	4.79	4.77	0.02
21	4.61	4.42	0.19
22	4.17	4.72	−0.55
23	4.91	4.91	0.00
24	4.2	4.68	−0.48
25	4.88	4.92	−0.04
26	4.55	4.59	−0.04
27	4.43	4.43	0.00
28	4.3	4.21	0.09
29	4.47	4.42	0.05
30	4.58	4.59	−0.01
31	4.25	4.29	−0.04
32	5.01	5.14	−0.13
33	4.94	4.80	0.14
34	5.01	4.97	0.04
35	4.37	4.35	0.02
36	4.78	4.85	−0.07

^a The underlined for the test set, and the rest for training.

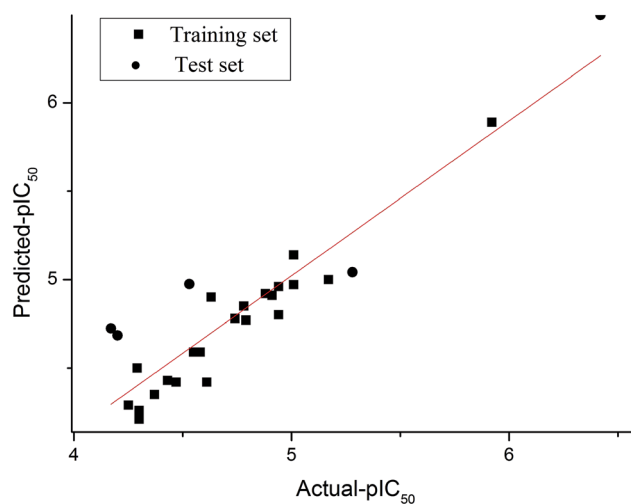


Fig. 6 Plot of experimental vs. predicted MMP-2 inhibitory activities of training set and test set.

Beijing, China). Thin layer chromatography (TLC) was performed on silica gel plates (Silica Gel 60 GF254) and visualized in UV light (254 nm). Column chromatography was performed using silica gel (200–300 mesh) eluting with ethyl acetate and petroleum ether.

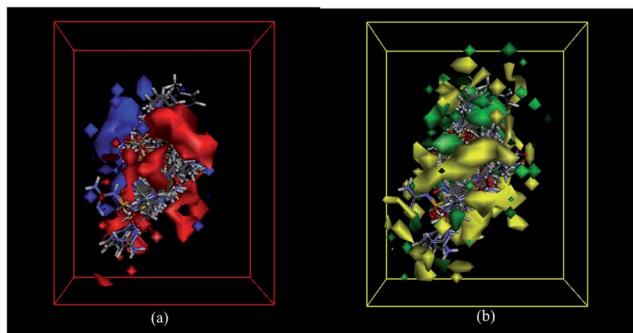


Fig. 7 (a) 3D QSAR model coefficients on electrostatic potential grids. Blue represents positive coefficients; red represents negative coefficients. (b) 3D QSAR model coefficients on van der Waals grids. Green represents positive coefficients; yellow represents negative coefficients.

4.2 General procedure for the synthesis of compounds 6–9

To a solution of sulfonamide derivatives (10 mmol) in ethanol (100 mL) was added salicylaldehyde (10 mmol). The reaction mixture was refluxed for 4 h, and monitored by TLC. After completion of the reaction, the precipitate was filtered and washed with ethanol for three times. The crude product was recrystallized from ethanol to furnish compounds 2–5. Without further purification, to a mixture of synthesized Schiff bases (10 mmol) in ethanol (100 mL), NaBH_4 (10 mmol) was slowly added in an ice bath with stirring. The reaction mixture was stirred for 4 h, then the solvent was concentrated and water (10 mL) was added. The product extraction was carried out with CH_2Cl_2 . Dried over Na_2SO_4 , the organic layer was then concentrated *in vacuo*. The residue was recrystallized from ethanol to afford pure compounds 6–9.

4.2.1 4-((2-Hydroxybenzyl)amino)benzenesulfonamide (6).³⁵

4.2.2 N-Carbamimidoyl-4-(2-hydroxybenzylamino)benzenesulfonamide (7). White crystal, yield 87.4%, m.p. 205–207 °C. ^1H NMR ($\text{DMSO}-d_6$, 300 MHz) δ : 9.62 (s, 1H, OH), 7.40 (d, 2H, $J = 8.8$ Hz, ArH), 7.34–7.28 (m, 3H, ArH), 7.11–7.08 (m, 1H, NH), 6.82 (s, 1H, ArH), 6.57 (s, 4H, NH_2 and NH), 6.36 (d, 2H, $J = 8.7$ Hz, ArH), 4.10 (s, 2H, CH_2).

4.2.3 N-(4-(2-Hydroxybenzylamino)phenylsulfonyl)acetamide (8). White crystal, yield 84.6%, m.p. 175–177 °C. ^1H NMR ($\text{DMSO}-d_6$, 300 MHz) δ : 11.70 (s, 1H, SO_2NH), 9.62 (s, 1H, OH), 7.55 (d, 2H, $J = 9.0$ Hz, ArH), 7.34–7.28 (m, 3H, ArH), 7.22 (t, 1H, $J = 6.0$ Hz, ArH), 7.13–7.11 (m, 1H, NH), 6.45 (d, 2H, $J = 8.8$ Hz, ArH), 4.15 (d, 2H, $J = 5.9$ Hz, CH_2), 1.86 (s, 3H, CH_3).

4.2.4 4-(2-Hydroxybenzylamino)-N-(4-methylpyrimidin-2-yl)benzenesulfonamide (9). White crystal, yield 85.2%, m.p. 208–201 °C. ^1H NMR ($\text{DMSO}-d_6$, 300 MHz) δ : 11.18 (s, 1H, SO_2NH), 9.62 (s, 1H, OH), 8.32 (d, 1H, $J = 5.1$ Hz, ArH), 7.34–7.27 (m, 3H, ArH), 7.09–7.04 (m, 2H, ArH), 6.90 (d, 1H, $J = 5.1$ Hz, NH), 6.42 (d, 2H, $J = 5.1$ Hz, ArH), 4.10 (d, 2H, $J = 5.8$ Hz, CH_2), 2.31 (s, 3H, CH_3).

4.3 General procedure for the synthesis of compounds 10–36

Triethylamine (10 mmol) was slowly added into a stirred solution of 6–9 (5 mmol), benzene sulfonyl chloride derivatives (10

mmol) in methanol (40 mL), DMF (5 mL). The reaction was stirred at ice bath for 10 h and monitored by TLC. After the completion of the reaction, the mixture was evaporated under reduced pressure to give a residue. Then the residue was purified by silica gel chromatography and recrystallized from ethanol to obtain pure compounds 10–36.

4.3.1 2-((4-Sulfamoylphenylamino)methyl)phenyl benzenesulfonate (10). White crystal, yield 52.2%, m.p. 140–141 °C. ^1H NMR ($\text{DMSO}-d_6$, 400 MHz) δ (ppm): 7.97 (d, 2H, $J = 7.4$ Hz, ArH), 7.89 (d, 1H, $J = 7.5$ Hz, ArH), 7.73 (d, 2H, $J = 7.8$ Hz, ArH), 7.47 (d, 2H, $J = 8.8$ Hz, NH_2), 7.34–7.26 (m, 3H, ArH), 7.10–7.08 (m, 1H, NH), 6.94 (m, 3H, ArH), 6.41 (d, 2H, $J = 8.7$ Hz, ArH), 4.13 (d, 2H, $J = 6.0$ Hz, CH_2). MS (ESI): 419.1 ($[\text{M} + \text{H}]^+$).

4.3.2 2-((4-Sulfamoylphenylamino)methyl)phenyl 4-methylbenzenesulfonate (11). White crystal, yield 58.0%, m.p. 122–124 °C. ^1H NMR ($\text{DMSO}-d_6$, 400 MHz) δ (ppm): 7.83 (d, 2H, $J = 8.3$ Hz, ArH), 7.53 (d, 2H, $J = 8.1$ Hz, ArH), 7.45 (d, 2H, $J = 8.8$ Hz, NH_2), 7.33–7.24 (m, 3H, ArH), 7.12–7.10 (m, 1H, NH), 6.93 (s, 3H, ArH), 6.38 (d, 2H, $J = 8.8$ Hz, ArH), 4.11 (d, 2H, $J = 6.0$ Hz, CH_2), 2.45 (s, 3H, CH_3). MS (ESI): 433.5 ($[\text{M} + \text{H}]^+$).

4.3.3 2-((4-Sulfamoylphenylamino)methyl)phenyl 4-nitrobenzenesulfonate (12). Yellow crystal, yield 54.2%, m.p. 166–168 °C. ^1H NMR ($\text{DMSO}-d_6$, 300 MHz) δ (ppm): 8.49 (d, 2H, $J = 8.7$ Hz, ArH), 8.26 (d, 2H, $J = 8.8$ Hz, ArH), 7.48 (d, 2H, $J = 8.5$ Hz, NH_2), 7.33–7.30 (m, 3H, ArH), 7.08–7.06 (m, 1H, NH), 6.91 (s, 3H, ArH), 6.50 (d, 2H, $J = 8.6$ Hz, ArH), 4.22 (d, 2H, $J = 5.8$ Hz, CH_2). MS (ESI): 464.1 ($[\text{M} + \text{H}]^+$).

4.3.4 2-((4-Sulfamoylphenylamino)methyl)phenyl 4-bromobenzenesulfonate (13). White crystal, yield 60.1%, m.p. 148–150 °C. ^1H NMR ($\text{DMSO}-d_6$, 300 MHz) δ (ppm): 7.96–7.86 (m, 4H, ArH), 7.48 (d, 2H, $J = 8.7$ Hz, NH_2), 7.34–7.28 (m, 3H, ArH), 7.11–7.10 (m, 1H, NH), 6.91 (m, 3H, ArH), 6.43 (d, 2H, $J = 8.7$ Hz, ArH), 4.15 (d, 2H, $J = 6.0$ Hz, CH_2). MS (ESI): 497.0 ($[\text{M} + \text{H}]^+$).

4.3.5 2-((4-Sulfamoylphenylamino)methyl)phenyl 4-chlorobenzenesulfonate (14). White crystal, yield 56.3%, m.p. 139–141 °C. ^1H NMR ($\text{DMSO}-d_6$, 300 MHz) δ (ppm): 7.97 (d, 2H, $J = 5.1$ Hz, ArH), 7.80 (d, 2H, $J = 5.1$ Hz, ArH), 7.47 (d, 2H, $J = 5.1$ Hz, NH_2), 7.32–7.29 (m, 3H, ArH), 7.09 (d, 1H, $J = 4.2$ Hz, NH), 6.91 (s, 3H, ArH), 6.43 (d, 2H, $J = 5.0$ Hz, ArH), 4.15 (d, 2H, $J = 3.5$ Hz, CH_2). MS (ESI): 454.0 ($[\text{M} + \text{H}]^+$).

4.3.6 2-((4-Sulfamoylphenylamino)methyl)phenyl 4-fluorobenzenesulfonate (15). White crystal, yield 49.7%, m.p. 148–150 °C. ^1H NMR ($\text{DMSO}-d_6$, 300 MHz) δ (ppm): 8.07–8.02 (m, 2H, ArH), 7.56 (t, 2H, $J = 8.7$ Hz, ArH), 7.47 (d, 2H, $J = 8.8$ Hz, NH_2), 7.32–7.28 (m, 3H, ArH), 7.12–7.07 (m, 1H, NH), 6.91 (s, 3H, ArH), 6.44 (d, 2H, $J = 8.8$ Hz, ArH), 4.15 (s, 2H, CH_2). MS (ESI): 437.1 ($[\text{M} + \text{H}]^+$).

4.3.7 2-((4-Sulfamoylphenylamino)methyl)phenyl 3-nitrobenzenesulfonate (16). Yellow crystal, yield 64.2%, m.p. 173–175 °C. ^1H NMR ($\text{DMSO}-d_6$, 300 MHz) δ (ppm): 8.66 (d, 1H, $J = 8.2$ Hz, ArH), 8.56 (t, $J = 1.8$ Hz, 1H), 8.41 (d, 1H, $J = 8.0$ Hz, ArH), 7.99 (t, 1H, $J = 8.1$ Hz, ArH), 7.47 (d, 2H, $J = 8.7$ Hz, NH_2), 7.35–7.29 (m, 3H, ArH), 7.12–7.09 (m, 1H, NH), 6.92 (s, 3H, ArH), 6.49 (d, 2H, $J = 8.8$ Hz, ArH), 4.22 (d, 2H, $J = 5.9$ Hz, CH_2). MS (ESI): 464.1 ($[\text{M} + \text{H}]^+$).

4.3.8 2-((4-(N-Carbamimidoylsulfamoyl)phenylamino)methyl)phenyl benzenesulfonate (17). White crystal, yield 50.1%, m.p.

254–257 °C. ^1H NMR (DMSO- d_6 , 400 MHz) δ (ppm): 7.97 (d, 2H, J = 8.4 Hz, ArH), 7.88 (t, 1H, J = 7.5 Hz, ArH), 7.72 (t, 2H, J = 7.9 Hz, ArH), 7.40 (d, 2H, J = 8.8 Hz, ArH), 7.34–7.28 (m, 3H, ArH), 7.11–7.08 (m, 1H, NH), 6.82 (s, 1H, ArH), 6.57 (s, 4H, NH₂ and NH), 6.36 (d, 2H, J = 8.7 Hz, ArH), 4.10 (s, 2H, CH₂). MS (ESI): 461.1 ([M + H]⁺).

4.3.9 2-((4-(*N*-Carbamimidoylsulfamoyl)phenylamino)methyl)phenyl 4-methylbenzenesulfonate (18). White crystal, yield 59.9%, m.p. 182–184 °C. ^1H NMR (DMSO- d_6 , 300 MHz) δ (ppm): 7.82 (d, 2H, J = 8.3 Hz, ArH), 7.51 (d, 2H, J = 8.2 Hz, ArH), 7.38 (d, 2H, J = 8.7 Hz, ArH), 7.31–7.26 (m, 3H, ArH), 7.12–7.09 (m, 1H, NH), 6.78 (t, 1H, J = 5.9 Hz, ArH), 6.54 (s, 4H, NH₂ and NH), 6.32 (d, 2H, J = 8.7 Hz, ArH), 4.07 (d, 2H, J = 6.0 Hz, CH₂), 2.43 (s, 3H, CH₃). MS (ESI): 475.1 ([M + H]⁺).

4.3.10 2-((4-(*N*-Carbamimidoylsulfamoyl)phenylamino)methyl)phenyl 4-nitrobenzenesulfonate (19). Yellow crystal, yield 58.5%, m.p. 132–134 °C. ^1H NMR (DMSO- d_6 , 300 MHz) δ (ppm): 8.49 (d, 2H, J = 8.8 Hz, ArH), 8.25 (d, 2H, J = 8.8 Hz, ArH), 7.40 (d, 2H, J = 8.6 Hz, ArH), 7.33–7.29 (m, 3H, ArH), 7.08–7.05 (m, 1H, NH), 6.80 (t, 1H, J = 5.7 Hz, ArH), 6.55 (s, 4H, NH₂ and NH), 6.43 (d, 2H, J = 8.7 Hz, ArH), 4.18 (d, 2H, J = 5.6 Hz, CH₂). MS (ESI): 506.1 ([M + H]⁺).

4.3.11 2-((4-(*N*-Carbamimidoylsulfamoyl)phenylamino)methyl)phenyl 4-bromobenzenesulfonate (20). White crystal, yield 41.9%, m.p. 108–110 °C. ^1H NMR (DMSO- d_6 , 400 MHz) δ (ppm): 7.94 (d, 2H, J = 8.7 Hz, ArH), 7.87 (d, 2H, J = 8.8 Hz, ArH), 7.40 (d, 2H, J = 8.6 Hz, ArH), 7.34–7.26 (s, 3H, ArH), 7.12–7.10 (m, 1H, NH), 6.85 (t, 1H, J = 6.1 Hz, ArH), 6.56 (s, 4H, NH₂ and NH), 6.34 (d, 2H, J = 8.7 Hz, ArH), 4.10 (d, 2H, J = 6.0 Hz, CH₂). MS (ESI): 539.1 ([M + H]⁺).

4.3.12 2-((4-(*N*-Carbamimidoylsulfamoyl)phenylamino)methyl)phenyl 4-chlorobenzenesulfonate (21). White crystal, yield 48.3%, m.p. 98–100 °C. ^1H NMR (DMSO- d_6 , 400 MHz) δ (ppm): 7.96 (d, 2H, J = 8.6 Hz, ArH), 7.79 (d, 2H, J = 8.7 Hz, ArH), 7.40 (d, 2H, J = 8.6 Hz, ArH), 7.33–7.28 (m, 3H, ArH), 7.12–7.09 (m, 1H, NH), 6.85 (t, 1H, J = 6.0 Hz, ArH), 6.56 (s, 4H, NH₂ and NH), 6.43 (d, 2H, J = 8.7 Hz, ArH), 4.11 (d, 2H, J = 6.0 Hz, CH₂). MS (ESI): 495.1 ([M + H]⁺).

4.3.13 2-((4-(*N*-Carbamimidoylsulfamoyl)phenylamino)methyl)phenyl 4-fluorobenzenesulfonate (22). White crystal, yield 46.4%, m.p. 112–114 °C. ^1H NMR (DMSO- d_6 , 400 MHz) δ (ppm): 8.06–8.02 (m, 2H, ArH), 7.59–7.54 (m, 2H, ArH), 7.39 (d, 2H, J = 8.8 Hz, ArH), 7.33–7.28 (m, 3H, ArH), 7.09–7.07 (m, 1H, NH), 6.85 (t, 1H, J = 6.0 Hz, ArH), 6.56 (s, 4H, NH₂ and NH), 6.36 (d, 2H, J = 8.7 Hz, ArH), 4.11 (d, 2H, J = 5.9 Hz, CH₂). MS (ESI): 479.1 ([M + H]⁺).

4.3.14 2-((4-(*N*-Carbamimidoylsulfamoyl)phenylamino)methyl)phenyl 3-nitrobenzenesulfonate (23). Yellow crystal, yield 61.1%, m.p. 214–216 °C. ^1H NMR (DMSO- d_6 , 400 MHz) δ (ppm): 8.68–8.65 (m, 1H, ArH), 8.56 (t, 1H, J = 2.0 Hz, ArH), 8.41–8.39 (m, 1H, ArH), 7.98 (t, 1H, J = 8.0 Hz, ArH), 7.39 (d, 2H, J = 8.8 Hz, ArH), 7.35–7.29 (m, 3H, ArH), 7.13–7.08 (m, 1H, NH), 6.82 (t, 1H, J = 5.8 Hz, ArH), 6.56 (s, 4H, NH₂), 6.42 (d, 2H, J = 8.8 Hz, ArH), 4.19 (d, 2H, J = 5.5 Hz, CH₂). MS (ESI): 506.1 ([M + H]⁺).

4.3.15 2-((4-(*N*-Acetylsulfamoyl)phenylamino)methyl)phenyl 4-methylbenzenesulfonate (24). White crystal, yield 55.7%, m.p. 120–122 °C. ^1H NMR (DMSO- d_6 , 400 MHz) δ (ppm): 11.70 (s, 1H,

SO₂NH), 7.82 (d, 2H, J = 8.3 Hz, ArH), 7.53–7.49 (m, 4H, ArH), 7.33–7.27 (m, 3H, ArH), 7.20 (t, 1H, J = 5.9 Hz, ArH), 7.13–7.10 (m, 1H, NH), 6.39 (d, 2H, J = 8.3 Hz, ArH), 4.10 (d, 2H, J = 5.8 Hz, CH₂), 2.43 (s, 3H, CH₃), 1.86 (s, 3H, CH₃). MS (ESI): 475.1 ([M + H]⁺).

4.3.16 2-((4-(*N*-Acetylsulfamoyl)phenylamino)methyl)phenyl 4-nitrobenzenesulfonate (25). Yellow crystal, yield 66.3%, m.p. 160–162 °C. ^1H NMR (DMSO- d_6 , 400 MHz) δ (ppm): 11.71 (s, 1H, SO₂NH), 8.47 (d, 2H, J = 8.9 Hz, ArH), 8.24 (d, 2H, J = 8.9 Hz, ArH), 7.54 (d, 2H, J = 8.9 Hz, ArH), 7.35–7.32 (m, 3H, ArH), 7.19 (t, 1H, J = 5.9 Hz, ArH), 7.09–7.07 (m, 1H, NH), 6.51 (d, 2H, J = 8.8 Hz, ArH), 4.19 (d, 2H, J = 5.8 Hz, CH₂), 1.86 (s, 3H, CH₃). MS (ESI): 506.1 ([M + H]⁺).

4.3.17 2-((4-(*N*-Acetylsulfamoyl)phenylamino)methyl)phenyl 4-bromobenzenesulfonate (26). White crystal, yield 59.2%, m.p. 190–193 °C. ^1H NMR (DMSO- d_6 , 400 MHz) δ (ppm): 11.70 (s, 1H, SO₂NH), 7.93–7.86 (m, 4H, ArH), 7.55 (d, 2H, J = 9.0 Hz, ArH), 7.36–7.30 (m, 3H, ArH), 7.22 (t, 1H, J = 5.9 Hz, ArH), 7.12–7.10 (m, 1H, NH), 6.45 (d, 2H, J = 9.0 Hz, ArH), 4.14 (d, 2H, J = 5.9 Hz, CH₂). MS (ESI): 538.0 ([M + H]⁺).

4.3.18 2-((4-(*N*-Acetylsulfamoyl)phenylamino)methyl)phenyl 4-chlorobenzenesulfonate (27). White crystal, yield 54.2%, m.p. 184–186 °C. ^1H NMR (DMSO- d_6 , 400 MHz) δ (ppm): 11.70 (s, 1H, SO₂NH), 7.96 (d, 2H, J = 8.7 Hz, ArH), 7.78 (d, 2H, J = 8.7 Hz, ArH), 7.55 (d, 2H, J = 9.0 Hz, ArH), 7.34–7.28 (m, 3H, ArH), 7.22 (t, 1H, J = 6.0 Hz, ArH), 7.13–7.11 (m, 1H, NH), 6.45 (d, 2H, J = 8.8 Hz, ArH), 4.15 (d, 2H, J = 5.9 Hz, CH₂), 1.86 (s, 3H, CH₃). MS (ESI): 495.0 ([M + H]⁺).

4.3.19 2-((4-(*N*-Acetylsulfamoyl)phenylamino)methyl)phenyl 4-fluorobenzenesulfonate (28). White crystal, yield 51.7%, m.p. 140–141 °C. ^1H NMR (DMSO- d_6 , 400 MHz) δ (ppm): 11.70 (s, 1H, SO₂NH), 8.07–8.03 (m, 2H, ArH), 7.58–7.54 (m, 4H, ArH), 7.35–7.31 (m, 3H, ArH), 7.22 (t, 1H, J = 6.0 Hz, ArH), 7.11–7.10 (m, 1H, NH), 6.48 (d, 2H, J = 8.7 Hz, ArH), 4.17 (d, 2H, J = 5.9 Hz, CH₂), 1.87 (s, 3H, CH₃). MS (ESI): 479.1 ([M + H]⁺).

4.3.20 2-((4-(*N*-Acetylsulfamoyl)phenylamino)methyl)phenyl 3-nitrobenzenesulfonate (29). Yellow crystal, yield 58.9%, m.p. 186–188 °C. ^1H NMR (DMSO- d_6 , 400 MHz) δ (ppm): 11.70 (s, 1H, SO₂NH), 8.64–8.62 (m, 1H, ArH), 8.56 (t, 1H, J = 1.9 Hz, ArH), 8.40 (d, 1H, J = 7.9 Hz, ArH), 7.97 (t, 1H, J = 8.1 Hz, ArH), 7.54 (d, 2H, J = 9.0 Hz, ArH), 7.38–7.31 (m, 3H, ArH), 7.18 (t, 1H, J = 5.8 Hz, ArH), 7.13–7.11 (m, 1H, NH), 6.51 (d, 2H, J = 8.8 Hz, ArH), 4.21 (d, 2H, J = 5.8 Hz, CH₂), 1.87 (s, 3H, CH₃). MS (ESI): 506.1 ([M + H]⁺).

4.3.21 2-((4-(*N*-(4-Methylpyrimidin-2-yl)sulfamoyl)phenylamino)methyl)phenyl benzenesulfonate (30). White crystal, yield 43.4%, m.p. 203–205 °C. ^1H NMR (DMSO- d_6 , 400 MHz) δ (ppm): 11.18 (s, 1H, SO₂NH), 8.32 (d, 1H, J = 5.1 Hz, ArH), 7.95 (d, 2H, J = 7.3 Hz, ArH), 7.85 (t, 1H, J = 7.5 Hz, ArH), 7.72–7.64 (m, 4H, ArH), 7.34–7.27 (m, 3H, ArH), 7.09–7.04 (m, 2H, ArH), 6.90 (d, 1H, J = 5.1 Hz, NH), 6.42 (d, 2H, J = 5.1 Hz, ArH), 4.10 (d, 2H, J = 5.8 Hz, CH₂), 2.31 (s, 3H, CH₃). MS (ESI): 511.1 ([M + H]⁺).

4.3.22 2-((4-(*N*-(4-Methylpyrimidin-2-yl)sulfamoyl)phenylamino)methyl)phenyl 4-methylbenzenesulfonate (31). White crystal, yield 48.5%, m.p. 184–186 °C. ^1H NMR (DMSO- d_6 , 400 MHz) δ (ppm): 11.21 (s, 1H, SO₂NH), 8.30 (d, 1H, J = 5.0 Hz,

ArH), 7.80 (d, 2H, $J = 8.2$ Hz, ArH), 7.63 (d, 2H, $J = 8.9$ Hz, ArH), 7.48 (d, 2H, $J = 8.1$ Hz, ArH), 7.33–7.24 (m, 3H, ArH), 7.10 (d, 1H, $J = 7.8$ Hz, ArH), 7.04 (t, 1H, $J = 5.5$ Hz, ArH), 6.88 (d, 1H, $J = 5.0$ Hz, NH), 6.37 (d, 2H, $J = 8.6$ Hz, ArH), 4.07 (d, 2H, $J = 5.8$ Hz, CH₂), 2.39 (s, 3H, CH₃), 2.29 (s, 3H, CH₃). MS (ESI): 525.1 ([M + H]⁺).

4.3.23 2-((4-(*N*-(4-Methylpyrimidin-2-yl)sulfamoyl)phenylamino)methyl)phenyl 4-nitrobenzenesulfonate (32). Yellow crystal, yield 61.9%, m.p. 235–237 °C. ¹H NMR (DMSO-*d*₆, 400 MHz) δ (ppm): 11.17 (s, 1H, SO₂NH), 8.46 (d, 2H, $J = 8.9$ Hz, ArH), 8.30 (d, 1H, $J = 5.1$ Hz, ArH), 8.23 (d, 2H, $J = 9.0$ Hz, ArH), 7.65 (d, 2H, $J = 9.0$ Hz, ArH), 7.31 (d, 3H, $J = 3.0$ Hz, ArH), 7.09–7.05 (m, 2H, ArH), 6.88 (d, 1H, $J = 5.1$ Hz, NH), 6.48 (d, 2H, $J = 8.8$ Hz, ArH), 4.15 (d, 2H, $J = 13.9$ Hz, CH₂), 2.29 (s, 3H, CH₃). MS (ESI): 556.1 ([M + H]⁺).

4.3.24 2-((4-(*N*-(4-Methylpyrimidin-2-yl)sulfamoyl)phenylamino)methyl)phenyl 4-bromobenzenesulfonate (33). White crystal, yield 44.5%, m.p. 192–194 °C. ¹H NMR (DMSO-*d*₆, 400 MHz) δ (ppm): 11.16 (s, 1H, SO₂NH), 8.30 (d, 1H, $J = 5.1$ Hz, ArH), 7.91–7.85 (m, 4H, ArH), 7.66 (d, 2H, $J = 8.9$ Hz, ArH), 7.34–7.27 (m, 3H, ArH), 7.11 (d, 1H, $J = 7.5$ Hz, ArH), 7.04 (t, 1H, $J = 5.9$ Hz, ArH), 6.88 (d, 1H, $J = 5.1$ Hz, NH), 6.42 (d, 2H, $J = 8.8$ Hz, ArH), 4.11 (d, 2H, $J = 5.9$ Hz, CH₂), 2.29 (s, 3H, CH₃). MS (ESI): 589.0 ([M + H]⁺).

4.3.25 2-((4-(*N*-(4-Methylpyrimidin-2-yl)sulfamoyl)phenylamino)methyl)phenyl 4-chlorobenzenesulfonate (34). White crystal, yield 51.8%, m.p. 198–200 °C. ¹H NMR (DMSO-*d*₆, 400 MHz) δ (ppm): 11.16 (s, 1H, SO₂NH), 8.30 (d, 1H, $J = 5.0$ Hz, ArH), 7.95 (d, 2H, $J = 8.8$ Hz, ArH), 7.75 (d, 2H, $J = 8.8$ Hz, ArH), 7.65 (d, 2H, $J = 8.9$ Hz, ArH), 7.34–7.27 (m, 3H, ArH), 7.11 (d, 1H, $J = 7.5$ Hz, ArH), 7.04 (t, 1H, $J = 5.8$ Hz, ArH), 6.88 (d, 1H, $J = 5.0$ Hz, NH), 6.42 (d, 2H, $J = 8.8$ Hz, ArH), 4.11 (d, 2H, $J = 5.9$ Hz, CH₂), 2.29 (s, 3H, CH₃). MS (ESI): 545.1 ([M + H]⁺).

4.3.26 2-((4-(*N*-(4-Methylpyrimidin-2-yl)sulfamoyl)phenylamino)methyl)phenyl 4-fluorobenzenesulfonate (35). White crystal, yield 48.6%, m.p. 215–217 °C. ¹H NMR (DMSO-*d*₆, 400 MHz) δ (ppm): 11.16 (s, 1H, SO₂NH), 8.30 (d, 1H, $J = 5.0$ Hz, ArH), 8.04–8.01 (m, 2H, ArH), 7.65 (d, 2H, $J = 8.9$ Hz, ArH), 7.53 (d, 2H, $J = 8.8$ Hz, ArH), 7.34–7.27 (m, 3H, ArH), 7.09 (d, 1H, $J = 7.5$ Hz, ArH), 7.04 (t, 1H, $J = 5.4$ Hz, ArH), 6.88 (d, 1H, $J = 5.0$ Hz, NH), 6.43 (d, 2H, $J = 8.8$ Hz, ArH), 4.12 (d, 2H, $J = 5.6$ Hz, CH₂), 2.29 (s, 3H, CH₃). MS (ESI): 529.1 ([M + H]⁺).

4.3.27 2-((4-(*N*-(4-Methylpyrimidin-2-yl)sulfamoyl)phenylamino)methyl)phenyl 3-nitrobenzenesulfonate (36). Yellow crystal, yield 56.3%, m.p. 208–210 °C. ¹H NMR (DMSO-*d*₆, 400 MHz) δ (ppm): 11.17 (s, 1H, SO₂NH), 8.63–8.61 (m, 1H, ArH), 8.56 (t, 1H, $J = 1.9$ Hz, ArH), 8.40 (d, 1H, $J = 7.7$ Hz, ArH), 8.32 (d, 1H, $J = 5.0$ Hz, ArH), 7.96 (t, 1H, $J = 8.0$ Hz, ArH), 7.65 (d, 2H, $J = 8.8$ Hz, ArH), 7.34–7.31 (m, 3H, ArH), 7.13–7.11 (m, 1H, ArH), 7.03 (t, 1H, $J = 5.1$ Hz, ArH), 6.90 (d, 1H, $J = 4.9$ Hz, NH), 6.48 (d, 2H, $J = 8.8$ Hz, ArH), 4.19 (d, 2H, $J = 5.8$ Hz, CH₂), 2.30 (s, 3H, CH₃). MS (ESI): 556.1 ([M + H]⁺).

4.4 Biological assays

4.4.1 MMP-2 inhibition assay.²⁰ First of all, the rhMMP-2 was diluted to 100 $\mu\text{g mL}^{-1}$ and activated with 1 mM APMA in

assay buffer. Afterwards, the reaction was incubated at 37 °C for 1 hour. Then the rhMMP-2 was diluted to 0.2 $\mu\text{g mL}^{-1}$ in assay buffer, while subsequently the substrate was diluted to 20 μM in assay buffer. To each well of a 96-well plate, 50 μL diluted rhMMP-2 was loaded along with 100 μL diverse concentration of compounds in test. The reaction was started by adding 50 μL of 20 μM substrate to each well. The samples were read in a fluorescence plate reader with Ex. = 320 nm and Em. = 405 nm, respectively, in kinetic mode for 5 minutes.

4.4.2 Antiproliferation activity.³⁶ The antiproliferation activities of the prepared compounds were evaluated using a standard (MTT)-based colorimetric assay with some modification. Cell lines were grown to log phase in DMEM supplemented with 10% fetal bovine serum, under a humidified atmosphere of 5% CO₂ at 37 °C. Cell suspensions were prepared and 100 μL per well dispensed into 96-well plates giving 10⁵ cells per well. The plates were returned to the incubator for 24 h to allow the cells to reattach. Subsequently, cells were treated with the target compounds at increasing concentrations in the presence of 10% FBS for 48 h. Then, cell viability was assessed by the conventional 3-(4,5-dimethylthiazol-2-yl)-2,5-diphenyltetrazolium bromide (MTT) reduction assay and carried out strictly according to the manufacturer instructions (Sigma). The absorbance (OD₅₇₀) was read on an ELISA reader (Tecan, Austria).

4.4.3 Cytotoxicity test.^{37,38} Cells were incubated in a 96-well plate at a density of 10⁵ cells per well with various concentrations of compounds for 48 h. For the cytotoxicity assay, 20 μL of MTT (5 mg mL⁻¹) was added per well 4 h before the end of the incubation. After removing the supernatant, 200 μL DMSO was added to dissolve the formazan crystals. The absorbance at λ 570 nm was read on an ELISA reader (Tecan, Austria).

4.4.4 Apoptosis assay.³⁹ Approximately 10⁵ cells per well were plated in a 24 well plate and allowed to adhere. Subsequently, the medium was replaced with fresh culture medium containing compounds **19** at final concentrations of 2, 8, 32 μM . Non-treated wells received an equivalent volume of ethanol (<0.1%). After 24 h, they were trypsinized, washed in PBS and centrifuged at 2000 rpm for 5 min. The pellet was then resuspended in 500 μL of staining solution (containing 5 μL AnnexinV-FITC and 5 μL PI in Binding Buffer), mixed gently and incubated for 15 min at room temperature in dark. The samples were then analyzed by a FACSCalibur flow cytometer (Becton Dickinson, San Jose, CA, USA).

4.5 Crystal structure determination

Crystal structure determination of compound **10** and **16** were carried out on a Nonius CAD4 diffractometer equipped with graphite-monochromated Mo-K α (0.7103 Å) radiation. The structures were solved by direct methods and refined on F^2 by full-matrix least-squares methods using SHELX-97[23]. All the non-hydrogen atoms were refined anisotropically. All the hydrogen atoms were placed in calculated position and were assigned fixed isotropic thermal parameters at 1.2 times the equivalent isotropic U of the atoms to which they are attached and allowed to ride on their respective parent atoms. The

contributions of these hydrogen atoms were included in the structure-factors calculations. The crystal data, data collection, and refinement parameter for the two compounds were listed in Table 1.

4.6 Experimental protocol of docking study

Molecular docking of compound **19** into the three dimensional X-ray structure of Matrix metalloproteinases (PDB code: 1QIB) was carried out using the Discovery Studio (version 3.5) as implemented through the graphical user interface DS-CDOCKER protocol. The three-dimensional structures of the aforementioned compounds were constructed using Chem. 3D ultra 12.0 software [Chemical Structure Drawing Standard; Cambridge Soft corporation, USA (2010)], then they were energetically minimized by using MMFF94 with 5000 iterations and minimum RMS gradient of 0.10. The crystal structures of protein complex were retrieved from the RCSB Protein Data Bank (<http://www.rcsb.org/pdb/home/home.do>). All bound waters and ligands were eliminated from the protein. The molecular docking was performed by inserting compound **19** into the binding pocket of MMP-2 based on the binding mode. Types of interactions of the docked protein with ligand-based pharmacophore model were analyzed after the end of molecular docking.

4.7 3D-QSAR²³

Ligand-based 3D-QSAR approach was performed by QSAR software of DS 3.5 (Discovery Studio 3.5, Accelrys, Co.Ltd). The training sets were composed of inhibitors with the corresponding pIC₅₀ values which were converted from the obtained IC₅₀ (μM), and test sets comprised compounds of data sets as list in Table 4. All the definition of the descriptors can be seen in the "Help" of DS 3.5 software and they were calculated by QSAR protocol of DS 3.5. The alignment conformation of each molecule was the one with lowest interaction energy in the docked results of CDOCKER. The predictive ability of 3D-QSAR modeling can be evaluated based on the cross-validated correlation coefficient, which qualifies the predictive ability of the models. Scrambled test (*Y* scrambling) was performed to investigate the risk of chance correlations. The inhibitory potencies of compounds were randomly reordered for 30 times and subject to leave-one-out validation test, respectively. The models were also validated by test sets, in which the compounds are not included in the training sets.

Acknowledgements

This work was supported by Natural Science Foundation of Jiangsu Province of China (no. BK20130554), and supported by "PCSIRT" (IRT1020).

References and notes

1 J. F. Woessner and H. Nagase, *Matrix Metalloproteinases and TIMPs*, Oxford University Press, New York, 2000.

- M. Whittaker, C. D. Floyd, P. Brown and A. J. Gearing, *Chem. Rev.*, 1999, **99**, 2735–2776.
- L. G. Monovich, R. A. Tommasi, R. A. Fujimoto, V. Blancuzzi, K. Clark, W. D. Cornell, R. Doti, J. Doughty, J. Fang and D. Farley, *J. Med. Chem.*, 2009, **52**, 3523–3538.
- A. D. Rowan, G. J. Litherland, W. Hui and J. M. Milner, *Expert Opinion on Therapeutic Targets*, 2008, **12**, 1–18.
- J. Hu, P. E. Van den Steen, Q.-X. A. Sang and G. Opendakker, *Nat. Rev. Drug Discovery*, 2007, **6**, 480–498.
- H. I. Roach, *Expert Opinion on Drug Discovery*, 2008, **3**, 475–486.
- C. M. Overall and C. López-Otín, *Nat. Rev. Cancer*, 2002, **2**, 657–672.
- G. Pochetti, R. Montanari, C. Gege, C. Chevrier, A. G. Taveras and F. Mazza, *J. Med. Chem.*, 2009, **52**, 1040–1049.
- V. Hugenberg, B. Riemann, S. Hermann, O. Schober, M. Schäfers, K. Szardenings, A. Lebedev, U. Gangadharmath, H. Kolb and J. Walsh, *J. Med. Chem.*, 2013, **56**, 6858–6870.
- I. Stamenkovic, *J. Pathol.*, 2003, **200**, 448–464.
- L. M. Coussens, B. Fingleton and L. M. Matrisian, *Science*, 2002, **295**, 2387–2392.
- R. P. Beckett and M. Whittaker, *Expert Opin. Ther. Pat.*, 1998, **8**, 259–282.
- R. P. Robinson, E. R. Laird, J. F. Blake, J. Bordner, K. M. Donahue, L. L. Lopresti-Morrow, P. G. Mitchell, M. R. Reese, L. M. Reeves and E. J. Stam, *J. Med. Chem.*, 2000, **43**, 2293–2296.
- S. Hanessian, N. Moitessier, C. Gauchet and M. Viau, *J. Med. Chem.*, 2001, **44**, 3066–3073.
- D. T. Puerta and S. M. Cohen, *Curr. Top. Med. Chem.*, 2004, **4**, 1551–1573.
- B. Fingleton, *Curr. Pharm. Des.*, 2007, **13**, 333–346.
- H. Matter and M. Schudok, *Curr. Opin. Drug Discovery Dev.*, 2004, **7**, 513–535.
- M. L. Rothenberg, A. R. Nelson and K. R. Hande, *Oncologist*, 1998, **3**, 271–274.
- E. Rosenbaum, M. Zahurak, V. Sinibaldi, M. A. Carducci, R. Pili, M. Laufer, T. L. DeWeese and M. A. Eisenberger, *Clin. Cancer Res.*, 2005, **11**, 4437–4443.
- D. Bissett, K. J. O'Byrne, J. Von Pawel, U. Gatzemeier, A. Price, M. Nicolson, R. Mercier, E. Mazabel, C. Penning and M. H. Zhang, *J. Clin. Oncol.*, 2005, **23**, 842–849.
- T. Steinmetzer, A. Schweinitz, A. Stürzebecher, D. Dönnecke, K. Uhland, O. Schuster, P. Steinmetzer, F. Müller, R. Friedrich and M. E. Than, *J. Med. Chem.*, 2006, **49**, 4116–4126.
- F. Hemmings, M. Farhan, J. Rowland, L. Banken and R. Jain, *Rheumatology*, 2001, **40**, 537–543.
- R. P. Beckett and M. Whittaker, *Expert Opinion on Therapeutic Patents*, 1998, **8**, 259–282.
- J. J. Li, J. Nahra, A. R. Johnson, A. Bunker, P. O'Brien, W.-S. Yue, D. F. Ortwine, C.-F. Man, V. Baragi and K. Kilgore, *J. Med. Chem.*, 2008, **51**, 835–841.
- M. Sawa, T. Tsukamoto, T. Kiyoi, K. Kurokawa, F. Nakajima, Y. Nakada, K. Yokota, Y. Inoue, H. Kondo and K. Yoshino, *J. Med. Chem.*, 2002, **45**, 930–936.

- 26 B. Pirard, *Drug Discovery Today*, 2007, **12**, 640–646.
- 27 D. Georgiadis and A. Yiotakis, *Bioorg. Med. Chem.*, 2008, **16**, 8781–8794.
- 28 M. Hidalgo and S. G. Eckhardt, *J. Natl. Cancer Inst.*, 2001, **93**, 178–193.
- 29 S. C. Burdette, C. J. Frederickson, W. Bu and S. J. Lippard, *J. Am. Chem. Soc.*, 2003, **125**, 1778–1787.
- 30 S. Larionov, Z. Savel'eva, R. Klevtsova, E. Uskov, L. Glinskaya, S. Popov and A. Tkachev, *Russ. J. Coord. Chem.*, 2011, **37**, 1–7.
- 31 N. Zhao, L. Chen, W. Ren, H. Song and G. Zi, *J. Organomet. Chem.*, 2012, **712**, 29–36.
- 32 E. A. Katayev and M. B. Schmid, *Dalton Trans.*, 2011, **40**, 2778–2786.
- 33 R. Reich, A. Hoffman, A. Veerendhar, A. Maresca, A. Innocenti, C. T. Supuran and E. Breuer, *J. Med. Chem.*, 2012, **55**, 7875–7882.
- 34 F. Molina, L. L. Johnson, D. F. Ortwine, A. Pavlovsky, J. R. Rubin, R. W. Skeeane, A. D. White, C. Humblet, D. J. Hupe and T. L. Blundell, *Croat. Chem. Acta.*, 1999, **72**, 575–591.
- 35 R. Suresh, D. Kamalakkannan, K. Ranganathan, R. Arulkumaran, R. Sundararajan, S. Sakthinathan, S. Vijayakumar, K. Sathiyamoorthi, V. Mala and G. Vanangamudi, *Spectrochim. Acta, Part A*, 2013, **101**, 239–248.
- 36 J. Sun, D.-D. Li, J.-R. Li, F. Fang, Q.-R. Du, Y. Qian and H.-L. Zhu, *Org. Biomol. Chem.*, 2013, **11**, 7676–7686.
- 37 T. Mosmann, *J. Immunol. Methods*, 1983, **65**, 55–63.
- 38 A. Monks, D. Scudiero, P. Skehan, R. Shoemaker, K. Paull, D. Vistica, C. Hose, J. Langley, P. Cronise and A. Vaigro-Wolff, *J. Natl. Cancer Inst.*, 1991, **83**, 757–766.
- 39 G. Le Bras, C. Radanyi, J.-F. Peyrat, J.-D. Brion, M. Alami, V. Marsaud, B. Stella and J.-M. Renoir, *J. Med. Chem.*, 2007, **50**, 6189–6200.